

# Fragmentation of single-particle strength around the doubly-magic nucleus $^{132}\text{Sn}$ and the position of the $0f_{5/2}$ proton-hole state in $^{131}\text{In}$

V. Vaquero,<sup>1,\*</sup> A. Jungclaus,<sup>1</sup> T. Aumann,<sup>2,3</sup> J. Tscheuschner,<sup>2</sup> E.V. Litvinova,<sup>4</sup> J. A. Tostevin,<sup>5</sup> H. Baba,<sup>6</sup> D. S. Ahn,<sup>6</sup> R. Avigo,<sup>7,8</sup> K. Boretzky,<sup>3</sup> A. Bracco,<sup>7,8</sup> C. Caesar,<sup>2,3</sup> F. Camera,<sup>7,8</sup> S. Chen,<sup>9,6</sup> V. Derya,<sup>10</sup> P. Doornenbal,<sup>6</sup> J. Endres,<sup>10</sup> N. Fukuda,<sup>6</sup> U. Garg,<sup>11</sup> A. Giaz,<sup>7</sup> M. N. Harakeh,<sup>3,12</sup> M. Heil,<sup>3</sup> A. Horvat,<sup>2</sup> K. Ieki,<sup>13</sup> N. Imai,<sup>14</sup> N. Inabe,<sup>6</sup> N. Kalantar-Nayestanaki,<sup>12</sup> N. Kobayashi,<sup>14</sup> Y. Kondo,<sup>15</sup> S. Koyama,<sup>14</sup> T. Kubo,<sup>6</sup> I. Martel,<sup>16</sup> M. Matsushita,<sup>17</sup> B. Million,<sup>8</sup> T. Motobayashi,<sup>6</sup> T. Nakamura,<sup>15</sup> N. Nakatsuka,<sup>6,2</sup> M. Nishimura,<sup>6</sup> S. Nishimura,<sup>6</sup> S. Ota,<sup>17</sup> H. Otsu,<sup>6</sup> T. Ozaki,<sup>15</sup> M. Petri,<sup>2</sup> R. Reifarth,<sup>18</sup> J.L. Rodríguez-Sánchez,<sup>19,3</sup> D. Rossi,<sup>2</sup> A. T. Saito,<sup>15</sup> H. Sakurai,<sup>6,14</sup> D. Savran,<sup>3</sup> H. Scheit,<sup>2</sup> F. Schindler,<sup>2,3</sup> P. Schrock,<sup>2</sup> D. Semmler,<sup>2</sup> Y. Shiga,<sup>13,6</sup> M. Shikata,<sup>15</sup> Y. Shimizu,<sup>6</sup> H. Simon,<sup>3</sup> D. Steppenbeck,<sup>6</sup> H. Suzuki,<sup>6</sup> T. Sumikama,<sup>6</sup> D. Symochko,<sup>2</sup> I. Syndikus,<sup>2</sup> H. Takeda,<sup>6</sup> S. Takeuchi,<sup>6</sup> R. Taniuchi,<sup>14</sup> Y. Togano,<sup>15</sup> J. Tsubota,<sup>15</sup> H. Wang,<sup>6</sup> O. Wieland,<sup>8</sup> K. Yoneda,<sup>6</sup> J. Zenihiro,<sup>6</sup> and A. Zilges<sup>10</sup>

<sup>1</sup>*Instituto de Estructura de la Materia, CSIC, E-28006 Madrid, Spain*

<sup>2</sup>*Institut für Kernphysik, Technische Universität Darmstadt, D-64289 Darmstadt, Germany*

<sup>3</sup>*GSI Helmholtzzentrum für Schwerionenforschung GmbH, D-64291 Darmstadt, Germany*

<sup>4</sup>*Department of Physics, Western Michigan University, Kalamazoo, MI 49008-5252, USA*

<sup>5</sup>*Department of Physics, University of Surrey, Guildford, Surrey GU2 7XH, United Kingdom*

<sup>6</sup>*RIKEN Nishina Center, 2-1 Hirosawa, Wako, 351-0198 Saitama, Japan*

<sup>7</sup>*Dipartimento di Fisica dell'Università degli Studi di Milano, I-20133 Milano, Italy*

<sup>8</sup>*INFN, Sezione di Milano, I-20133 Milano, Italy*

<sup>9</sup>*School of Physics and State Key Laboratory of Nuclear Physics and Technology, Peking University, Beijing 100871, China*

<sup>10</sup>*Institut für Kernphysik, Universität zu Köln, D-50937 Köln, Germany*

<sup>11</sup>*Department of Physics, University of Notre Dame, Notre Dame, Indiana 46556, USA*

<sup>12</sup>*KVI-CART, Zernikelaan 25, NL-9747 AA Groningen, The Netherlands*

<sup>13</sup>*Department of Physics, Rikkyo University, Tokyo 171-8501, Japan*

<sup>14</sup>*Department of Physics, The University of Tokyo, Tokyo 113-0033, Japan*

<sup>15</sup>*Department of Physics, Tokyo Institute of Technology, Tokyo 152-8551, Japan*

<sup>16</sup>*Departamento de Física Aplicada, Universidad de Huelva, E-21071 Huelva, Spain*

<sup>17</sup>*Center for Nuclear Study, The University of Tokyo, Tokyo 113-0033, Japan*

<sup>18</sup>*Institut für Kernphysik, Goethe University Frankfurt, Frankfurt, Germany*

<sup>19</sup>*Universidad de Santiago de Compostela, E-15782 Santiago de Compostela, Spain*

(Dated: December 2, 2019)

Spectroscopic factors of neutron-hole and proton-hole states in  $^{131}\text{Sn}$  and  $^{131}\text{In}$ , respectively, were measured using one-nucleon removal reactions from doubly-magic  $^{132}\text{Sn}$  at relativistic energies. For  $^{131}\text{In}$ , a 2910(50)-keV  $\gamma$  ray was observed for the first time and tentatively assigned to a decay from a  $5/2^-$  state at 3275(50) keV to the known  $1/2^-$  level at 365 keV. The spectroscopic factors determined for this new excited state and three other single-hole states provide first evidence for a strong fragmentation of single-hole strength in  $^{131}\text{Sn}$  and  $^{131}\text{In}$ . The experimental results are compared to theoretical calculations based on the relativistic particle-vibration coupling model and to experimental information for single-hole states in the stable doubly-magic nucleus  $^{208}\text{Pb}$ .

One of the main pillars for understanding nuclear structure is the nuclear shell model, in which nucleons occupy single-particle orbitals under the influence of an average potential created by the interactions among all nucleons. Its predictive power was first demonstrated 70 years ago when the naive independent particle shell-model description was able to explain the large energy gaps, that appear in nuclei for some particular values of the number of protons and neutrons (magic numbers), with the inclusion of a strong attractive spin-orbit force [1,2]. In this picture, the occupation probabilities for the single-particle and single-hole states in the odd neighbors of a good doubly-magic nucleus, near the

Fermi surface, should be unity. However, for the stable magic nucleus  $^{208}\text{Pb}$  it is experimentally established that several single-particle states show a significant degree of depletion [3,4]. The description of fragmentation of single-particle strengths near the Fermi-surface is typically the realm of the nuclear shell-model. In addition, short-range correlations displace a fraction of strength to much higher energies [5,6], while coupling to collective vibrations drives additional fragmentation and the removal of strength from states close to the Fermi surface [7,8]. Due to the low excitation energy of the octupole  $3^-$  state at 2.61 MeV and the absence of positive parity states below 4 MeV, it is mainly the strong octupole coupling between the high-spin intruder orbital  $nl_j$  and its  $n(\ell-3)_{j-3}$  partner in each of the four quadrants around  $^{208}\text{Pb}$  which is responsible for the fragmen-

\* email: victor.vaquero@csic.es

tation. Later on, extended calculations including also the coupling to the giant resonances were presented [9]. Finally, very sophisticated calculations within (i) a relativistic particle-vibration coupling (PVC) model based on covariant density functional theory [10,11] and (ii) a fully self-consistent PVC approach within the framework of Skyrme energy density functional theory [12] have been performed which describe the experimental spectroscopic factors (SF) of single-particle levels around  $^{208}\text{Pb}$  reasonably well.

For the neutron-rich doubly-magic  $^{132}\text{Sn}$ , experimental information is much more scarce. The excitation energies of several single-particle states are still experimentally unknown and SF have only been measured for some neutron states in  $^{131,133}\text{Sn}$  employing transfer reactions with a low-energy radioactive  $^{132}\text{Sn}$  beam [13–16]. Since the collective octupole state in  $^{132}\text{Sn}$  has a much higher excitation energy of 4.35 MeV, as compared to the  $3^-$  state in  $^{208}\text{Pb}$  (2.61 MeV), and both this  $3^-$  and the first excited  $2^+$  state show significantly smaller collectivity [17], one may expect the single-particle strength around  $^{132}\text{Sn}$  to be less fragmented as compared to  $^{208}\text{Pb}$ .

In this Letter, we report on the measurement of the spectroscopic factors of the  $1d_{5/2}$  and  $0g_{7/2}$  neutron-hole states in  $^{131}\text{Sn}$  and the  $1p_{3/2}$  and  $0f_{5/2}$  proton-hole states in  $^{131}\text{In}$  using one-nucleon removal reactions at relativistic energies. For the first time, the  $\gamma$  decay of the  $0f_{5/2}$  state in  $^{131}\text{In}$  has been observed thus completing the set of proton-hole states in the  $Z=28-50$  major shell. The experimental results will be compared to both theoretical work and experimental information in the  $^{208}\text{Pb}$  region.

The experiment was performed at the Radioactive Isotope Beam Factory (RIBF), operated by the RIKEN Nishina Center and the Center for Nuclear Study of the University of Tokyo. A primary beam of  $^{238}\text{U}$  at 345 MeV/u with an intensity of 12 pnA bombarded a 4-mm thick beryllium target located at the entrance of the BigRIPS fragment separator [18]. Fission fragments around  $^{132}\text{Sn}$  were selected and purified employing the  $B\rho-\Delta E-B\rho$  method. Then, the atomic number ( $Z$ ) and the mass-over-charge ratio ( $A/q$ ) of each ion were determined using the  $\Delta E-B\rho$ -TOF method [19] before impinging on a 335(34) mg/cm<sup>2</sup> liquid helium reaction target [20]. Reaction products were identified in the ZeroDegree spectrometer [18] using again the  $\Delta E-B\rho$ -TOF method. Fig. 1(a) shows the particle identification plot of the ZeroDegree spectrometer for the  $^{132}\text{Sn}$  secondary beam impinging on the helium target with an energy of 203 MeV/u.

To detect  $\gamma$  radiation emitted in the decay of excited states of the reaction products, an array consisting of two different types of detectors was placed around the target: 96 NaI(Tl) scintillator crystals of the DALI2 spectrometer [21] covering polar angles  $\theta=50^\circ-150^\circ$  and eight large-volume LaBr<sub>3</sub>:Ce scintillator detectors of the HECTOR<sup>+</sup> array [22] at  $\theta=30^\circ$ . All detectors were calibrated using  $^{60}\text{Co}$ ,  $^{88}\text{Y}$  and Cm-C sources yielding intrinsic energy resolutions (FWHM) and photo-peak efficiencies of

6.5%/6.4% (NaI) and 3.1%/0.9% (LaBr<sub>3</sub>) for the 1.836-MeV  $\gamma$  ray emitted by the stationary  $^{88}\text{Y}$  source. The excellent time resolution of the LaBr<sub>3</sub> detectors allowed to distinguish the prompt  $\gamma$  radiation from the background due to particles which reached the detectors with a delay of 1-2 ns (see Fig. 1(b)). The Doppler-corrected  $\gamma$ -ray spectra ( $\beta=0.556$  at mid-target) measured with these detectors therefore exhibit a much better peak-to-background ratio as compared to the corresponding NaI spectra, see Fig. 1(c)-(f).

Before inspecting Fig. 1 in more detail, it is helpful to consider the reaction mechanism used here to populate excited states. The projectile  $^{132}\text{Sn}$  is a doubly-magic nucleus with  $N=82$  and  $Z=50$ . The removal of one neutron (proton) from an orbital of the completely filled  $N=50-82$  ( $Z=28-50$ ) major shell populates the corresponding neutron-hole (proton-hole) state in  $^{131}\text{Sn}$  ( $^{131}\text{In}$ ). Except for the  $0f_{5/2}$  proton-hole state in  $^{131}\text{In}$ , all these levels are known and their decay branches well established [23–29]. All decays which proceed via the emission of a  $\gamma$  ray with an energy above the set detection threshold of 900 keV should be observable in the present experiment. These are the 1655-keV and 2434-keV  $\gamma$  rays emitted in the decay of the  $1d_{5/2}$  and  $0g_{7/2}$  neutron-hole states in  $^{131}\text{Sn}$  and the 988-keV  $\gamma$  ray from the decay of the  $1p_{3/2}$  proton-hole state in  $^{131}\text{In}$ .

All three expected  $\gamma$ -ray peaks are clearly visible in the spectra shown in Figs. 1(c)-(f). In addition, a  $\gamma$ -ray transition in  $^{131}\text{In}$  with an energy of 2910(50) keV is observed for the first time and in both nuclei additional  $\gamma$  strength is present at energies above 3.5 MeV. Based on the arguments presented above, the 2910-keV  $\gamma$ -ray transition is assigned to the decay of the  $0f_{5/2}$  proton-hole state in  $^{131}\text{In}$ . Assuming an  $E2$  decay to the  $1/2^-$  state at 365 keV [29], an excitation energy of 3275(50) keV is tentatively assigned to the first excited  $5/2^-$  state in  $^{131}\text{In}$ . To understand the origin of the broad distribution of  $\gamma$  strength observed at high energy in both  $^{131}\text{Sn}$  and  $^{131}\text{In}$ , it has to be considered that a fraction of the  $^{132}\text{Sn}$  ions may reach the reaction target in the  $8_1^+$  isomeric state which is sufficiently long-lived ( $T_{1/2}=2.080(17)\ \mu\text{s}$  [30]) to survive the flight through the BigRIPS separator. One-nucleon removal from this excited state ( $E_x=4.85$  MeV), which is dominated by the  $\nu f_{7/2} h_{11/2}^{-1}$  configuration [31], will populate a large number of closely-lying three-quasi-particle states in  $^{131}\text{Sn}$  and  $^{131}\text{In}$  at excitation energies above 3.5 MeV [25, 26, 29, 32–34]. It is assumed that the decay of these states is responsible for the additional  $\gamma$  strength in the spectra shown in Figs. 1(c)-(f).

To determine exclusive one-nucleon removal cross sections to individual excited states, the experimental spectra were fitted by the sum of the detector responses to the observed  $\gamma$  rays simulated using GEANT4 [35] and a smooth background function. The resulting values are listed in Table I, together with the measured inclusive cross sections and theoretical values obtained using eikonal reaction theory and assuming full occupancy of all orbitals in the  $Z=28-50$  and  $N=50-82$  shells. The

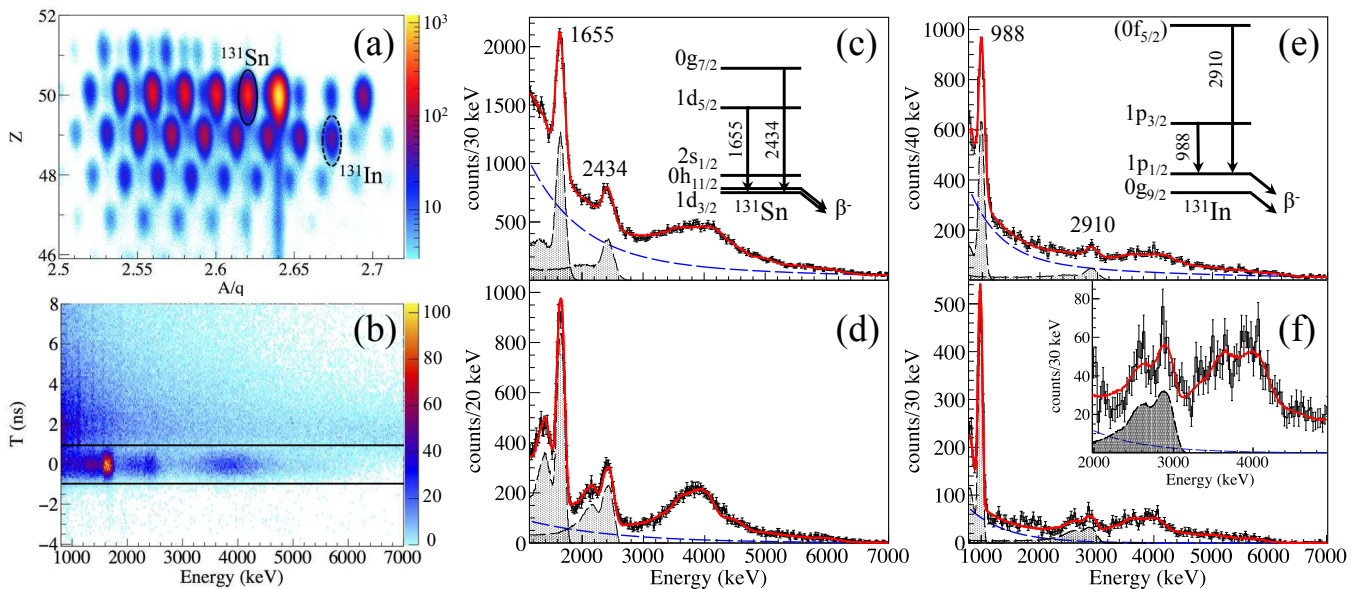


FIG. 1. (a) ZeroDegree particle identification plot for the  $^{132}\text{Sn}$  beam impinging on the helium reaction target. (b)  $\gamma$ -ray energy vs. time matrix for  $^{131}\text{Sn}$  measured with the LaBr<sub>3</sub> detectors. Doppler-corrected  $\gamma$ -ray spectra of  $^{131}\text{Sn}$  populated via one-neutron removal from  $^{132}\text{Sn}$  measured with (c) the NaI and (d) the LaBr<sub>3</sub> detectors. (e), (f) Same as (c), (d) for  $^{131}\text{In}$  populated via one-proton removal. In (c)-(f) the fit to the experimental spectrum (red solid line) is the sum of the background (blue dashed line) and the simulated response functions for the observed transitions (filled curves). In (c), (e) only events with multiplicity  $M_\gamma=1$  are considered in order to reduce the background. The insets in (c) and (e) show the level schemes of  $^{131}\text{Sn}$  and  $^{131}\text{In}$ , respectively.

knockout reaction description follows Refs. [36,37], except that the target, that removes the nucleon from the projectile in fast, surface-grazing collisions, is  $^4\text{He}$ . The absorptive nucleon-target interaction responsible for this process incorporates the  $^4\text{He}$  size through its one-body density [37]. Before SF can be extracted from a comparison of measured and calculated exclusive cross sections, various corrections have to be applied. First, the contribution from events, in which the projectile is excited to high excitation energies and evaporates a neutron, must be subtracted from the measured inclusive cross section for  $^{131}\text{Sn}$ ,  $\sigma_{incl}=120(15)$  mb. INCL calculations [38,39], that reproduce experimental inclusive cross sections for neutron removal from several  $N=83$  isotones [40], suggest this contribution is  $\approx 23\%$ . Assuming a relative uncertainty of 100% for this contribution, an inclusive direct neutron-removal cross section of  $\sigma_{incl}^{1n}=92(30)$  mb is obtained. Secondly, from the inclusive cross sections, we obtain quenching factors  $R_s=\sigma_{incl}^{exp}/\sigma_{incl}^{th}$  of 0.6(2) and 0.30(5) for the one-neutron and one-proton removal reactions, respectively. Furthermore, taking into account the effective separation-energy differences of  $\Delta S=S_n-S_p=7.68$  MeV for  $^{131}\text{Sn}$  and  $\Delta S=S_p-S_n=9.29$  MeV for  $^{131}\text{In}$  (with  $S_p/S_n$  being the proton/neutron-separation energy), these values are in qualitative agreement with the systematics established in Ref. [41] for lighter nuclei. For the following discussion of the fragmentation of hole strength in  $^{131}\text{Sn}$  and  $^{131}\text{In}$  relative SF normalized to the experimentally determined inclusive cross sections

are used. Thirdly, as discussed above, a fraction of removal events are from the  $8^+$  isomeric state. To estimate this fraction  $F$  it is assumed that removal from the  $8^+$  isomer always gives rise to the emission of one  $\gamma$  ray with energy above 3.5 MeV. Consistent values of  $F=13(3)\%$  and  $F=11(3)\%$  were deduced for  $^{131}\text{Sn}$  and  $^{131}\text{In}$ , respectively. Mindful of this assumption, a relative error of 100%, i.e. a value of  $F=12(12)\%$ , is used in the following. Finally, spectroscopic factors can be calculated using  $S_{exp}=\sigma_{excl}/[\sigma_{th}\cdot R_s\cdot(1-F)]$ , see Table I.

Figure 2 summarizes the experimental information concerning SF of single-particle states in the odd neighbors of  $^{132}\text{Sn}$  and  $^{208}\text{Pb}$ . We omit here the single-proton nuclei  $^{133}\text{Sb}$  and  $^{209}\text{Bi}$  since no experimental information on SF is available for  $^{133}\text{Sb}$ . Since the pioneering work of Blomqvist [61], it is well known that there is a close resemblance between the shell structures around these two doubly-magic nuclei. Each  $^{132}\text{Sn}$  orbital with quantum numbers  $n\ell_j$  has its counterpart with quantum numbers  $n(\ell+1)_{j+1}$  around  $^{208}\text{Pb}$ . Figure 2 suggests that this analogy also holds for the spectroscopic factors. The large values measured in Refs. [13,14] for the  $1f_{7/2}$ ,  $2p_{3/2}$ ,  $2p_{1/2}$ , and  $1f_{5/2}$  single-neutron states in  $^{133}\text{Sn}$  are in nice agreement with those measured for the corresponding orbitals in  $^{209}\text{Pb}$  (see Fig. 2(a)). Similarly, the reduced values for the  $1d_{5/2}$  and  $0g_{7/2}$  neutron-hole states in  $^{131}\text{Sn}$  and the  $1p_{3/2}$  and  $0f_{5/2}$  proton-hole states

TABLE I. Excitation energies ( $E_x$ ), theoretical single-particle ( $\sigma_{sp}$ ) and total ( $\sigma_{th}$ ) one-nucleon removal cross sections, measured exclusive cross sections ( $\sigma_{excl}$ ), and experimental spectroscopic factors ( $S_{exp}$ ) for the single-particle states  $n\ell_j$  in  $^{131}\text{Sn}$  and  $^{131}\text{In}$ .

$E_x$ (keV)	$n\ell_j$	$\sigma_{sp}$ (mb)	$\sigma_{th}$ (mb)	$\sigma_{excl}$ (mb)	$S_{exp}$
$^{131}\text{Sn}$					
0	$1d_{3/2}$	6.8	27.1	-	-
65	$0h_{11/2}$	4.7	55.9	-	-
332	$2s_{1/2}$	7.1	14.3	-	-
1655	$1d_{5/2}$	5.8	35.0	12.1(19)	0.65(26)
2434	$0g_{7/2}$	2.8	22.4	5.4(9)	0.46(18)
>3500				11.8(9)	
Inclusive cross sections:		$\sigma_{th}=154.6$ mb, $\sigma_{exp}=120(15)$ mb $R_s=0.6(2)$			
$^{131}\text{In}$					
0	$0g_{9/2}$	3.1	30.8	-	-
365	$1p_{1/2}$	3.2	6.4	-	-
1353	$1p_{3/2}$	3.1	12.4	2.3(5)	0.70(21)
3275(50)	$(0f_{5/2})$	1.7	10.3	0.68(14)	0.25(7)
>3500				2.0(3)	
Inclusive cross sections:		$\sigma_{th}=60.0$ mb, $\sigma_{exp}=18(3)$ mb $R_s=0.30(5)$			

in  $^{131}\text{In}$ , determined in the present work, are all in line with the experimental findings for their counterparts in the  $^{208}\text{Pb}$  region (see Figs. 2(b) and 2(c)). Comparison of the spectroscopic factors deduced from different direct reactions, low-energy transfer in Refs. [13,14,42-60] and intermediate-energy nucleon removal here, is justified since, in each case, the cross sections are dictated by the same single-particle overlaps near the nuclear surface [62]. As discussed earlier, the depletion of some single-particle states in the  $^{208}\text{Pb}$  core, for example the  $1f_{7/2}$  state in  $^{207}\text{Pb}$ , has been ascribed to the effects of particle-vibration coupling [8,9], in particular to the  $3_1^-$  state in the  $^{208}\text{Pb}$  core. In a recent work, a relativistic PVC model based on covariant density functional theory treated simultaneously the coupling to all  $2^+$ ,  $3^-$ ,  $4^+$ ,  $5^-$  and  $6^+$  states of the core up to an excitation energy of 15 MeV [11]. The calculated spectroscopic factors are included in Fig. 2 as dashed lines. A very good overall agreement with experiment is observed, while some relatively minor discrepancies may point out to missing higher-order correlations in the current version of the model. To investigate the origin of the depletion in the nine cases in which reduced SF were both measured and calculated, additional calculations were performed in which only couplings to either all  $2^+$  or all  $3^-$  states were considered. The results are summarized in Table II. For the  $0j_{15/2}$  level in  $^{209}\text{Pb}$  (the energy of the corresponding  $0i_{13/2}$  state in  $^{133}\text{Sn}$  is still unknown), the  $1d_{5/2}/1f_{7/2}$  levels in  $^{131}\text{Sn}/^{207}\text{Pb}$  and the  $1p_{3/2}/1d_{5/2}$  levels in  $^{131}\text{In}/^{207}\text{Tl}$ , the calculations clearly show that it is the coupling to the  $3^-$  states which leads to the reduc-

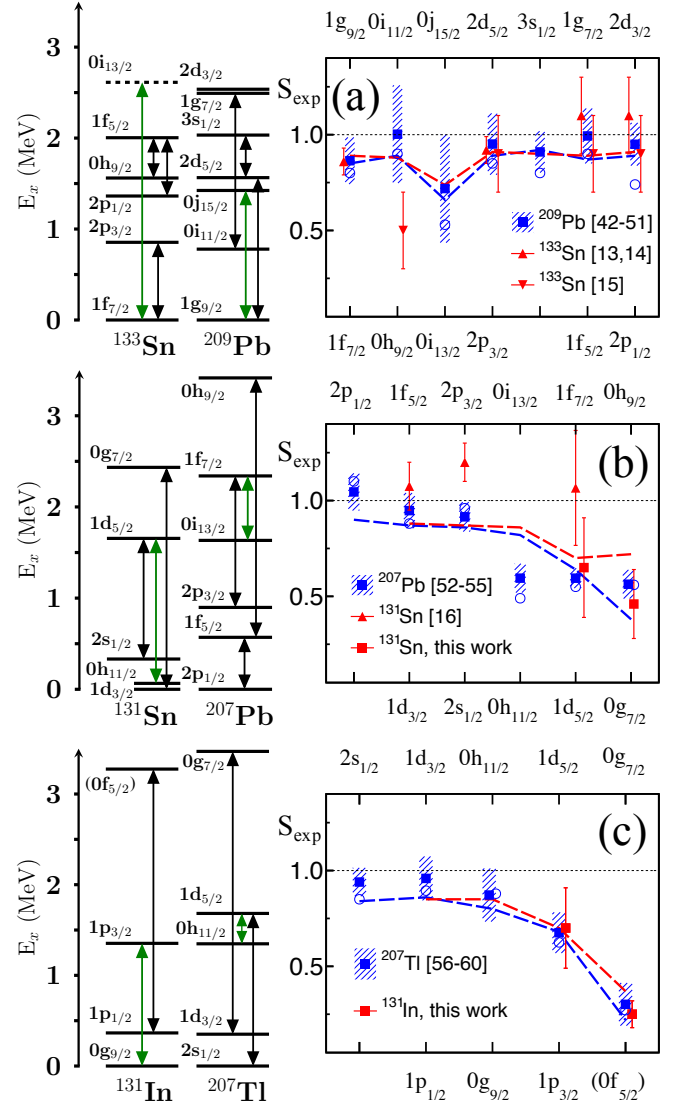


FIG. 2. Experimental spectroscopic factors of (a) single-neutron states in  $^{133}\text{Sn}$  and  $^{209}\text{Pb}$ , (b) neutron-hole states in  $^{131}\text{Sn}$  and  $^{207}\text{Pb}$  and (c) proton-hole states in  $^{131}\text{In}$  and  $^{207}\text{Tl}$  compared to calculations using the relativistic PVC model (dashed lines) [11]. At the top (bottom) axis the  $n(\ell+1)j_{+1}$  ( $n\ell_j$ ) orbitals around  $^{208}\text{Pb}$  ( $^{132}\text{Sn}$ ) are listed. For the  $^{208}\text{Pb}$  core, average literature values with their standard deviation (squares and hatched areas) as well as the most recent measurements (open circles) are included [42-60]. On the left, the single-particle states are shown. Green (black) arrows connect states with  $\Delta\ell=\Delta j=3$  ( $\Delta\ell=\Delta j=2$ ).

tion of the spectroscopic factor. In all cases the calculations predict that more than 95% of the single-particle strength is concentrated in only two states, indicating that actually only the coupling to the first  $3^-$  state is relevant. This finding agrees with the qualitative expectation. For example, the mixing of the  $0j_{15/2}$  level in  $^{209}\text{Pb}$  with the  $15/2^-$  member of the  $1g_{9/2}\otimes 3_1^-$  multiplet is expected to be stronger than that of the  $1g_{9/2}$  level with the  $9/2^+$  member of the  $0j_{15/2}\otimes 3_1^-$  multiplet, be-



TABLE II. Theoretical spectroscopic factors obtained considering the coupling to all vibrational states with spins of  $2^+$ ,  $3^-$ ,  $4^+$ ,  $5^-$ ,  $6^+$  up to an excitation energy of 15 MeV,  $S_{all}$ , to all  $2^+$  states,  $S_{2^+}$ , and to all  $3^-$  states,  $S_{3^-}$ , in the same energy range for selected orbitals in the neighbors of  $^{208}\text{Pb}$  and  $^{132}\text{Sn}$  (compare Fig. 2 and see text for details). The experimental values are included for comparison.

$^{208}\text{Pb}$ neighbors					$^{132}\text{Sn}$ neighbors				
orbital	$S_{all}$	$S_{2^+}$	$S_{3^-}$	$S_{exp}$	orbital	$S_{all}$	$S_{2^+}$	$S_{3^-}$	$S_{exp}$
$0j_{15/2}$	0.66	0.98	0.64	0.72(28)	$0i_{13/2}$	0.74	0.96	0.73	-
$1f_{7/2}$	0.64	0.95	0.68	0.60(5)	$1d_{5/2}$	0.70	0.93	0.76	0.65(26)
$1d_{5/2}$	0.68	0.95	0.75	0.68(11)	$1p_{3/2}$	0.71	0.94	0.79	0.70(21)
$0h_{9/2}$	0.38	0.80	0.83	0.56(8)	$0g_{7/2}$	0.72	0.81	0.72	0.46(18)
$0g_{7/2}$	0.23	0.40	0.51	0.30(11)	$0f_{5/2}$	0.36	0.33	0.79	0.25(7)

cause in the first case the energy difference between the two states of equal spin is much smaller.

For the  $0g_{7/2}/0h_{9/2}$  and  $0f_{5/2}/0g_{7/2}$  states in the one-hole nuclei  $^{131}\text{Sn}/^{207}\text{Pb}$  and  $^{131}\text{In}/^{207}\text{Tl}$ , the calculations indicate a more complex situation (see Table II) which results in a much stronger fragmentation of the single-particle strength. Considering the single-particle energies (compare Fig. 2), a coupling to the  $2^+$  states of the cores can be expected to play a major role here since all these levels lie 2.8-3.1 MeV above their  $n(\ell-2)_{j-2}$  counterparts, which means that the unperturbed  $n\ell_j$  single-hole states are close in energy to the  $n(\ell-2)_{j-2}\otimes 2^+$  multiplets. Indeed, reduced SF are obtained in the calculations which only consider coupling to  $2^+$  states. In addition, however, all four states are also close in energy to the equal-spin member of the *intruder* $\otimes 3^-$  multiplet. Therefore, coupling to the  $3^-$  states may also be important as confirmed by the calculations. Note that in the one-neutron nuclei  $^{133}\text{Sn}$  and  $^{209}\text{Pb}$  the situation is different. Here, the intruder state lies above its  $n(\ell-3)_{j-3}$

partner and, as a consequence, the *intruder* $\otimes 3^-$  multiplet is far away in energy from any state it could possibly mix with. In addition, the coupling to  $2^+$  states is much less favorable in these cases (see Fig. 2). This may explain why in these two nuclei only the intruder states are expected to have reduced spectroscopic factors.

To conclude, we reported the observation of the decay of a new excited state with an energy of 3275(50) keV in  $^{131}\text{In}$ , populated via one-proton removal from a doubly-magic  $^{132}\text{Sn}$  beam and tentatively assigned as the  $0f_{5/2}$  proton-hole state. In addition, measured spectroscopic factors of the  $1d_{5/2}$  and  $0g_{7/2}$  neutron-hole states in  $^{131}\text{Sn}$  and the  $1p_{3/2}$  and  $0f_{5/2}$  proton-hole states in  $^{131}\text{In}$  were reported and compared to their analog states in  $^{207}\text{Pb}$  and  $^{207}\text{Tl}$  and to a state-of-the-art relativistic PVC model. While the coupling to the first excited  $3^-$  states in the core nuclei  $^{132}\text{Sn}$  and  $^{208}\text{Pb}$  has been identified as the main origin for the reduced spectroscopic factors measured for the  $1d_{5/2}/1f_{7/2}$  single-particle states in  $^{131}\text{Sn}/^{207}\text{Pb}$  and the  $1p_{3/2}/1d_{5/2}$  levels in  $^{131}\text{In}/^{207}\text{Tl}$ , the coupling to more than one collective state, i.e. more complex coupling scenarios, are responsible for the strong fragmentation and the small measured spectroscopic factors in the case of the  $0g_{7/2}/0h_{9/2}$  states in  $^{131}\text{Sn}/^{207}\text{Pb}$  and the  $0f_{5/2}/0g_{7/2}$  levels in  $^{131}\text{In}/^{207}\text{Tl}$ .

We thank the staff of the RIKEN accelerator team for supplying a primary  $^{238}\text{U}$  beam with high intensity. This work was supported by the Spanish Ministerio de Economía y Competitividad under contract No. FPA2017-84756-C4-2-P, the DFG via Sonderforschungsbereich SFB 1245, the GSI-TU Darmstadt cooperation agreement and the US-NSF Career Grant PHY-1654379. J.A.T. acknowledges support of the Science and Technology Facilities Council (UK) grant ST/L005314/1.

- 
- [1] M. G. Mayer, *Phys. Rev.* **75**, 1969 (1949).  
[2] O. Haxel, J. H. D. Jensen, and H. E. Suess, *Phys. Rev.* **75**, 1766 (1949).  
[3] E. N. M. Quint *et al.*, *Phys. Rev. Lett.* **57**, 186 (1986).  
[4] M. C. Mermaz *et al.*, *Phys. Rev. C* **37**, 1942 (1988).  
[5] W. Dickhoff and C. Barbieri, *Progress in Particle and Nuclear Physics* **52**, 377 (2004).  
[6] L. Lapikás, *Nuclear Physics A* **553**, 297 (1993).  
[7] A. Bohr and B. Mottelson, *Nuclear Structure*, Vol. I (Benjamin, 1969).  
[8] I. Hamamoto, *Physics Reports* **10**, 63 (1974).  
[9] R. Majumdar, *Phys. Rev. C* **42**, 631 (1990).  
[10] E. Litvinova and P. Ring, *Phys. Rev. C* **73**, 044328 (2006).  
[11] E. V. Litvinova and A. V. Afanasjev, *Phys. Rev. C* **84**, 014305 (2011).  
[12] L.-G. Cao, G. Colò, H. Sagawa, and P. F. Bortignon, *Phys. Rev. C* **89**, 044314 (2014).  
[13] K. L. Jones *et al.*, *Nature (London)* **465**, 454.  
[14] K. L. Jones *et al.*, *Phys. Rev. C* **84**, 034601 (2011).  
[15] J. M. Allmond *et al.*, *Phys. Rev. Lett.* **112**, 172701 (2014).  
[16] R. Orlandi *et al.*, *Physics Letters B* **785**, 615 (2018).  
[17] D. Rosiak *et al.*, *Phys. Rev. Lett.* **121**, 252501 (2018).  
[18] T. Kubo *et al.*, *Prog. Theor. Exp. Phys.* **2012**, 03C003 (2012).  
[19] N. Fukuda *et al.*, *Nucl. Inst. Meth. B* **317**, 323 (2013).  
[20] H. Ryuto *et al.*, *Nucl. Instrum. Methods Phys. Res., Sect. A* **555**, 1 (2005).  
[21] S. Takeuchi *et al.*, *Nucl. Instrum. Methods Phys. Res., Sect. A* **763**, 596 (2014).  
[22] A. Giaz *et al.*, *Nucl. Instrum. Methods Phys. Res., Sect. A* **729**, 910 (2013).  
[23] L. E. De Geer and G. B. Holm, *Phys. Rev. C* **22**, 2163 (1980).  
[24] B. Fogelberg and J. Blomqvist, *Physics Letters B* **137**, 20 (1984).  
[25] B. Fogelberg and J. Blomqvist, *Nuclear Physics A* **429**, 205 (1984).  
[26] B. Fogelberg *et al.*, *Phys. Rev. C* **70**, 034312 (2004).

- [27] A. Kankainen *et al.*, *Phys. Rev. C* **87**, 024307 (2013).
- [28] J. Taprogge *et al.*, *Phys. Rev. Lett.* **112**, 132501 (2014).
- [29] J. Taprogge *et al.*, *The European Physical Journal A* **52**, 347 (2016).
- [30] K. Kawade *et al.*, *Zeitschrift für Physik A Atoms and Nuclei* **308**, 33 (1982).
- [31] G. Colò, P. F. Bortignon, and G. Bocchi, *Phys. Rev. C* **95**, 034303 (2017).
- [32] P. Bhattacharyya *et al.*, *Phys. Rev. Lett.* **87**, 062502 (2001).
- [33] R. Dunlop *et al.*, *Phys. Rev. C* **99**, 045805 (2019).
- [34] M. Górska *et al.*, *Physics Letters B* **672**, 313 (2009).
- [35] S. Agostinelli *et al.*, *Nucl. Instrum. Methods Phys. Res., Sect. A* **506**, 250 (2003).
- [36] J. Tostevin, *Nuclear Physics A* **682**, 320 (2001).
- [37] P. Hansen and J. Tostevin, *Annual Review of Nuclear and Particle Science* **53**, 219 (2003), <https://doi.org/10.1146/annurev.nucl.53.041002.110406>.
- [38] A. Boudard, J. Cugnon, J.-C. David, S. Leray, and D. Mancusi, *Phys. Rev. C* **87**, 014606 (2013).
- [39] J. L. Rodríguez-Sánchez, J.-C. David, D. Mancusi, A. Boudard, J. Cugnon, and S. Leray, *Phys. Rev. C* **96**, 054602 (2017).
- [40] V. Vaquero *et al.*, *Physics Letters B* **795**, 356 (2019).
- [41] J. A. Tostevin and A. Gade, *Phys. Rev. C* **90**, 057602 (2014).
- [42] M. Dost, W. Hering, and W. R. Smith, *Nuclear Physics A* **93**, 357 (1967).
- [43] G. Muehlehner, A. S. Poltorak, W. C. Parkinson, and R. H. Bassel, *Phys. Rev.* **159**, 1039 (1967).
- [44] G. Crawley, B. Rao, and D. Powell, *Nuclear Physics A* **112**, 223 (1968).
- [45] C. Ellegaard, J. Kantele, and P. Vedelsby, *Nuclear Physics A* **129**, 113 (1969).
- [46] A. Jeans, W. Darcey, W. Davies, K. Jones, and P. Smith, *Nuclear Physics A* **128**, 224 (1969).
- [47] J. J. van der Merwe and G. Heymann, *Zeitschrift für Physik A Hadrons and nuclei* **220**, 130 (1969).
- [48] R. Casten, E. Cosman, E. Flynn, O. Hansen, P. Keaton, N. Stein, and R. Stock, *Nuclear Physics A* **202**, 161 (1973).
- [49] D. Kovar, N. Stein, and C. Bockelman, *Nuclear Physics A* **231**, 266 (1974).
- [50] R. Tickle and W. Gray, *Nuclear Physics A* **247**, 187 (1975).
- [51] T. K. Roy and S. Mukherjee, *Journal of Physics G: Nuclear Physics* **13**, 1239 (1987).
- [52] S. Smith, P. Roos, C. Moazed, and A. Bernstein, *Nuclear Physics A* **173**, 32 (1971).
- [53] W. A. Lanford and G. M. Crawley, *Phys. Rev. C* **9**, 646 (1974).
- [54] J. Guillot, J. Van de Wiele, H. Langevin-Joliot, E. Gerlic, J. P. Didelez, G. Duhamel, G. Perrin, M. Buenerd, and J. Chauvin, *Phys. Rev. C* **21**, 879 (1980).
- [55] M. Matoba, K. Yamaguchi, K. Kurohmaru, O. Iwamoto, S. Widodo, A. Nohtomi, Y. Uozumi, T. Sakae, N. Koori, T. Maki, and M. Nakano, *Phys. Rev. C* **55**, 3152 (1997).
- [56] W. C. Parkinson, D. L. Hendrie, H. H. Duhamel, J. Mahoney, J. Saundinos, and G. R. Satchler, *Phys. Rev.* **178**, 1976 (1969).
- [57] D. Royer, M. Arditì, L. Bimbot, H. Doubre, N. Frascaria, J. Garron, and M. Riou, *Nuclear Physics A* **158**, 516 (1970).
- [58] P. D. Barnes, E. R. Flynn, G. J. Igo, and D. D. Armstrong, *Phys. Rev. C* **1**, 228 (1970).
- [59] H. Langevin-Joliot, E. Gerlic, J. Guillot, and J. van de Wiele, *Journal of Physics G: Nuclear Physics* **10**, 1435 (1984).
- [60] P. Grabmayr, A. Mondry, G. J. Wagner, P. Woldt, G. P. A. Berg, J. Lisantti, D. W. Miller, H. Nann, P. P. Singh, and E. J. Stephenson, *Journal of Physics G: Nuclear and Particle Physics* **18**, 1753 (1992).
- [61] J. Blomqvist, CERN Report No. 81-09, CERN, Geneva, 1981 (unpublished), p. 535.
- [62] A. Mutschler *et al.*, *Phys. Rev. C* **93**, 034333 (2016).